ORIGINAL ARTICLE

Experience Shapes the Development of Neural Substrates of Face Processing in Human Ventral Temporal Cortex

Golijeh Golarai[1], Alina Liberman[3] and Kalanit Grill-Spector[1,2]

[1]Department of Psychology, Stanford University, [2]Neuroscience Institute, Stanford University, Stanford, CA 94305-213, USA and [3]University of California, Berkeley, 94720 CA, USA

Address correspondence to Golijeh Golarai. Department of Psychology, Jordan Hall (Bldg. 420), Stanford University, Stanford, CA 94305-213, USA. Email: ggolarai@stanford.edu

Abstract

In adult humans, the ventral temporal cortex (VTC) represents faces in a reproducible topology. However, it is unknown what role visual experience plays in the development of this topology. Using functional magnetic resonance imaging in children and adults, we found a sequential development, in which the topology of face-selective activations across the VTC was matured by age 7, but the spatial extent and degree of face selectivity continued to develop past age 7 into adulthood. Importantly, own- and other-age faces were differentially represented, both in the distributed multivoxel patterns across the VTC, and also in the magnitude of responses of face-selective regions. These results provide strong evidence that experience shapes cortical representations of faces during development from childhood to adulthood. Our findings have important implications for the role of experience and age in shaping the neural substrates of face processing in the human VTC.

Key words: development, face-processing, fusiform gyrus, high-level vision, ventral temporal cortex

Introduction

In adult humans, the ventral temporal cortex (VTC) responds to complex visual stimuli, such as faces, objects, and scenes, in a characteristic spatial organization that is reliable with respect to cortical gyri and sulci. These visual stimuli are represented in two complementary manners across the VTC, namely as (1) distributed patterns of activation across the entire VTC, containing information about the categorical membership of visual stimuli (Haxby et al. 2001; Kriegeskorte et al. 2008), and as (2) regions that respond more strongly to stimuli of a particular category than others, such as face-selective regions along the fusiform gyrus (FG, Kanwisher et al. 1997). These face-selective regions constitute the peaks of distributed face representations across the VTC (Haxby et al. 2001). Furthermore, there is a reliable correspondence between large-scale anatomical landmarks and functional topology across the VTC, in terms of both regional selectivity and distributed responses to visual stimuli (Weiner and Grill-Spector 2010; Nasr et al. 2011; Weiner et al. 2014). This correspondence between structure and function suggests that anatomical constraints may play an important role in shaping the functional organization of VTC, supporting the idea that this functional topology develops early. In contrast, converging evidence suggests that face-selective regions in the FG undergo a slow childhood development (Gathers et al. 2004; Aylward et al. 2005; Golarai et al. 2007, 2010; Scherf et al. 2007, 2012; Peelen et al. 2009; Cantlon et al. 2011), which continues well into the teens (Golarai et al. 2010) and is associated with an age-related increase in the spatial extent of face-selective activations. These findings have raised the possibility that an experience-dependent developmental process shapes the functional organization of VTC. However, two key questions remain. First, does the spatial organization of distributed responses to faces or other objects change during childhood? Second, does visual experience play a role in shaping the development of the distributed representations or face-selective regions in VTC?

To elucidate the development of functional topology of VTC in response to faces and objects, we tested the hypothesis that childhood development involves qualitative changes in the spatial topology of distributed responses to visual categories. Supporting this possibility, some evidence suggests that the cortical location of face-selective regions is different in young children compared with adults. For example, one study found that face-selective regions are located outside of the FG in 5–8 year olds (Gathers et al. 2004), and another study reported their absence in 5–8 year olds (Scherf et al. 2007). According to this hypothesis, qualitative developments in the overall functional topology may lead to age-related changes in the distributed representations of visual categories. However, other studies support a second hypothesis, in which the topology of VTC responses remains qualitatively stable after age 7. This hypothesis is based on evidence that the anatomical location of face-, object-, and scene-selective regions in children as young as 7 years old were similar to adults (Golarai et al. 2007, 2010; Scherf et al. 2007, 2012; Peelen et al. 2009; Cantlon et al. 2011). This hypothesis predicts that the spatial extent and magnitude of face selectivity increase with age, but these developments minimally alter the large-scale functional topology of the VTC, as face-selective regions constitute only a small portion of the surface area of the VTC. A third possibility is that in the absence of large-scale topological differences across age groups, even subtle developmental changes in the functional topology might alter the category information content of distributed responses in the VTC.

Another goal of our study was to examine the role of experience in shaping the functional organization of the VTC and particularly face processing. This poses a challenge, as both cumulative experience and maturational processes contribute to development, and it is not feasible to manipulate children's experience with faces over long periods. Instead, we sought to use normal variations in the social milieu, and thus exposure to different types of faces during the life-span to test the effects of experience on the development of face processing in the VTC (Cassia et al. 2009; Harrison and Hole 2009; Hills and Lewis 2011).

One possibility is that relatively recent experience with own-age faces plays a key role in shaping the functional organization of the VTC. Supporting a role for experience, a recent study of juvenile macaque infero-temporal cortex found a spatial segregation of regions selective for natural versus cartoon faces after intense training with cartoon faces (Srihasam et al. 2012, 2014). In humans, experience with own-age faces may show more prominent effects in adults, who have many more years of experience with adult faces, than in children whose own-age cohorts span only a few years. Neurally, these experience-dependent effects may manifest in the VTC in 3 ways that are not mutually exclusive: (1) as different distributed responses to own- versus other-age faces, (2) in the spatial segregation of regions selective for own- versus other-age faces, and (3) in different amplitudes of responses to own- versus other-age faces in regions with overlapping selectivity for both face subtypes.

A second possibility is that maturation dominates the functional development of VTC. This hypothesis predicts that age-related changes in the functional organization or response properties of the VTC will be similar for own- and other-age faces.

A third possibility is that both experience-dependent and experience-independent neural mechanisms shape the functional properties of the VTC, where each type of mechanism differentially shapes the functional attributes of distributed responses across the VTC or local responses of category-selective regions. This hypothesis predicts that some representations in the VTC are shaped by experience-dependent mechanisms and, others by experience-independent mechanisms.

Here, we used functional magnetic resonance imaging (fMRI) to examine the development of functional organization in VTC from childhood to adulthood and elucidate the contributions of maturation and experience-dependent mechanisms. Children (ages 7–11 years old) and adults (ages 18–40 years old) underwent fMRI as they viewed images of own- and other-age faces, cars and novel objects, as well as scenes and textures (Fig. 1A). Across the VTC, we examined the development of distributed multivoxel patterns (MVPs) of responses to faces, objects, and scenes, as well as the development of face-selective regions in the FG. To test the effects of recent versus cumulative experience on the development of VTC, we compared responses to subtypes of faces (own- vs. other-ages) and objects (cars vs. novel objects), with which subjects had varying levels of prior experience. We expected that maturation would lead to age-related changes independent of stimulus subtype, while experience-related changes would lead to interactions between age of subject and age of faces (or types of objects), depending on the duration of subjects' prior experience.

Materials and Methods

Subjects

A total of 25 children, ages 7–11 years, and 13 adults, ages 18–40 years, participated in our experiments. Thirteen of 25 children and 1 of 13 adults were excluded from data analysis due to excessive motion during fMRI. The remaining subjects were matched across age groups on the quality of blood–oxygen-level-dependent (BOLD) signals (Fig. B–G). Thus, data from 12 children (ages 7–11, 7 females), and 12 adults (ages 18–40, 6 females) are reported in this study.

Subjects had normal or corrected vision with no past or current neurological or psychiatric conditions. Children were recruited from the Palo Alto school districts through advertisements in school newspapers, and attended local public schools at the time of study. Adult subjects were university affiliates and were not engaged with children in their daily work at the time of the experiment. Only 2 of 12 adult participants were parents (living with their children who were >5 year olds). Informed consent was obtained according to the requirements of the Panel on Human Subjects in Medical Research at Stanford University. Children were invited to a practice session to exercise motion control in a simulated scanner environment. All subjects were acclimated to the scanner before fMRI by first participating in anatomical MRI.

Scanning

MRI data were acquired on a 3 Tesla whole-body General Electric Signa MRI scanner (General Electric, Milwaukee, WI) at the Lucas Imaging Center at Stanford University.

Structural MRI
Using a head coil we acquired 4 whole-brain anatomical scans using 3D Fast SPGR, 166 sagittal slices, 0.938 mm × 0.938 mm, 1.5 mm slice thickness, and 256 × 256 image matrix.

Functional MRI
Using an 8-channel surface coil (Nova Medical, www.novamedical.com), we acquired functional images applying T_2^*-sensitive gradient echo spiral pulse sequence (Glover 1999) across 32 slices,
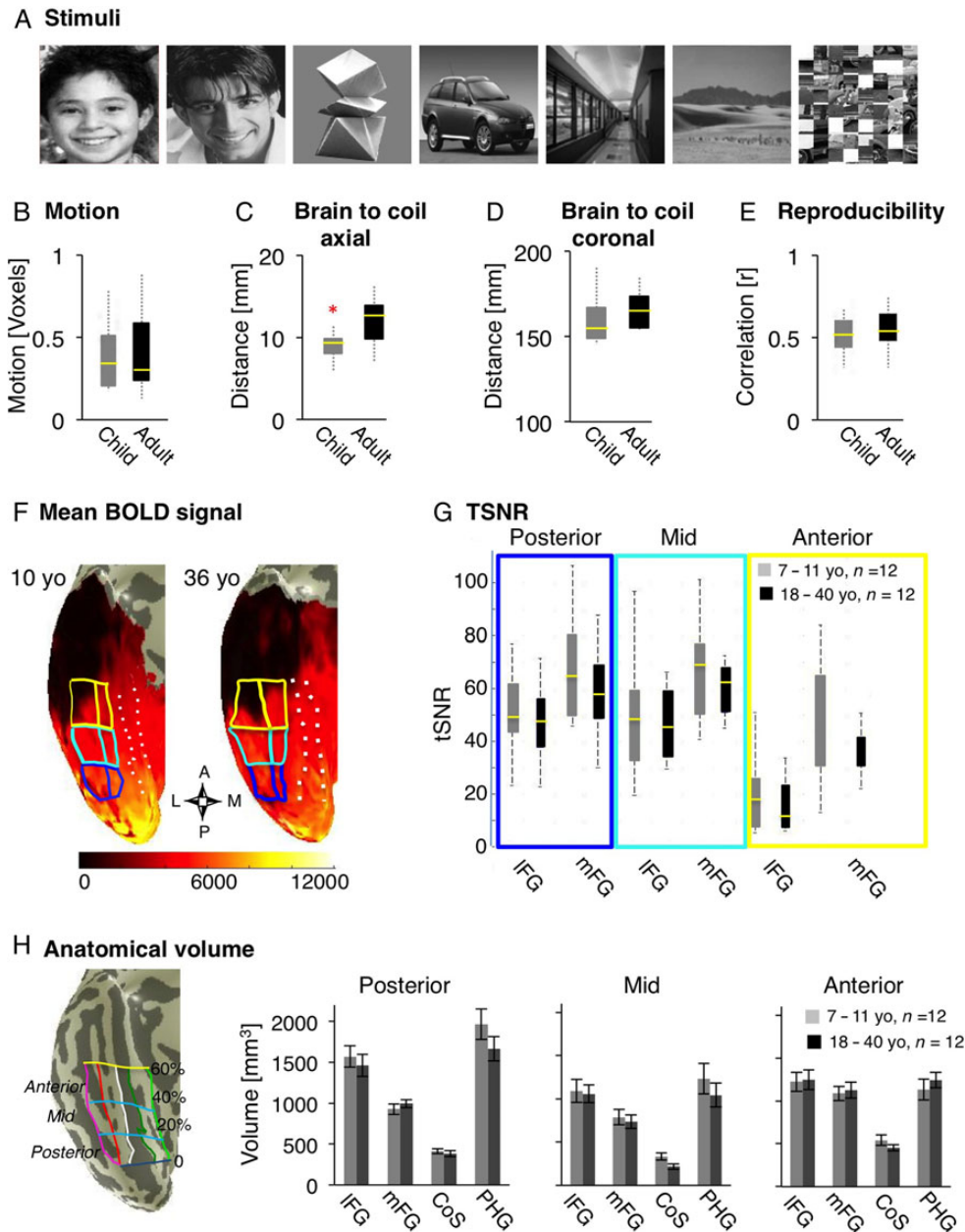
Figure 1. Visual stimuli, controls for BOLD data quality, and measurements of anatomical volume across age-groups. (A) Sample stimuli of each of the visual categories and subtypes that subjects viewed during fMRI. (B–G) Measures of parameters that may affect the quality of BOLD signals in 12 children (gray) and 12 adults (black). Each boxplot represents the median (yellow line), the 25% and 75% quartiles (length of box), minimum and maximum values (whiskers). (B) Motion: total motion across 2 fMRI runs was matched between age groups. (C) Distance between brain to coil in the axial plane: the shortest distance between the occipital pole and the outer edge of the skull along the largest axial in each subject's anatomical scan. Asterisk: significant between age group difference $P = 0.01$ due to children's thinner skulls. (D) Distance in the coronal plane: the distance between the outer ears along the widest coronal axis in each subject's anatomical scan, is an estimate of subject's fit within the head coil and distance of brain to coil in the coronal plane. Age groups were not different. (E) Reproducibility: correlation between MVPs of response to different images of the same subcategory across 2 runs of localizer, averaged across all subcategories for each subject. Age groups were not different. (F) Mean BOLD signal (arbitrary scanner units) over 2 runs visualized on the surface of VTC in inflated brains from representative 10- and 36-years old participants. The compass below shows the orientation of VTC (A: anterior, P: posterior, M: medial, L: lateral). Lighter colors represent higher mean BOLD signals and dark regions represent low BOLD signals. The ear canal susceptibility artifact in the anterior VTC is black and tends to be larger in adults than in children. Solid lines: boundaries of 6 anatomically defined ROIs along the posterior (blue), mid (cyan), and anterior (yellow) fusiform gyrus (FG). Dashed lines: boundaries of the collateral sulcus (CoS) and parahippocampal gyrus (PHG). (G) Time series signal-to-noise ratio (tSNR) was measured in each of the anatomical ROIs of the posterior, mid, and anterior FG. Data are plotted separately for the lateral and mid FG (lFG, mFG), in each anatomical ROI and for each age group. Mean tSNRs within these partitions were not statistically different across age groups. (H) Anatomical volume. Left: 12 anatomical partitions of the VTC are plotted on the surface of VTC from a representative 10-year-old subject. Vertical lines show the divisions of VTC in the lateral to medial direction: the lateral boundary of the occipito temporal sulcus (OTS, magenta), the bisecting axis of mid fusiform sulcus mid fusiform sulcus (MFS, red) which divides the FG into lFG and mFG, the lateral and medial boundaries of CoS (white and dark green), and the medial boundary of the PHG and lingual gyrus (light green). The posterior boundary of the VTC was defined as the fundus of the posterior transverse CoS (ptCoS). Horizontal lines show the 20%, 40% and 60% of the length of the cortical surface from the ptCoS to the anterior pole on coronal sections, creating 3 compartments of VTC: posterior: dark blue (0 to 20%), mid: cyan (20–40%), and anterior: yellow (40–60%). Right: The volume of gray matter in each of the 4 lateral-medial partitions of the posterior, mid, and anterior VTC averaged in each hemisphere and across children (gray, $n = 12$) and adults (black, $n = 12$). There were no significant between group differences in the size of the anatomical partitions. Error bars indicate between subjects SEM.

oriented perpendicular to the calcarine sulcus and extending from the occipital pole to the anterior temporal lobe (time repetition [TR] = 2000 ms, time echo = 30 ms, flip angle = 76°, field of view = 200 mm, resolution: 3.125 × 3.125 × 3 mm). Applying the same slice prescription, we acquired anatomical T_1-weighted images to register each subject's functional data to their whole-brain anatomy.

Visual Presentation
Images were projected onto a screen and viewed via a mirror mounted on the fMRI coil (visual angle = 15°). Images were presented and responses were recorded via a Macbook Pro using Matlab (Mathworks) and Psychtoolbox (www.psychtoolbox.org).

Visual Stimuli
Stimuli consisted of gray-scale images of frontal view of male faces (school aged children, and young adults, all faces were Caucasian, with a uniform happy or neutral expression, minimal facial hair, without glasses or jewelry), novel objects (abstract sculptures), common cars (all modern makes), indoor scenes, outdoor scenes (all devoid of people, animals, or salient objects), and scrambled images (created by randomly scrambling pictures into 225, 8 × 8 pixel squares, Fig. 1A).

Face images were collected from advertising web sites for models, and were matched for distinctiveness and attractiveness by 4 adult observers. We used male faces based on the assumption that most children have lower exposure to male adults in the role of nonparental caretakers or school teachers. Additionally, we aimed to reduce gender effects, as some behavioral studies suggest that females have better face recognition memory compared with males due to their selectively better recognition memory for female faces (Lewin and Herlitz 2002).

Pixel-wise similarity (Grill-Spector et al. 1999) of image subtypes between the 2 runs were not different across face stimuli (child faces: 0.30 ± 0.01; adult faces: 0.30 ± 0.01) and scenes (indoor scenes 0.36 ± 0.01, outdoor scenes 0.35 ± 0.01; mean ± SEM), but car images were more similar to each other than images of novel objects were to each other (cars: 0.42 ± 0.01, novel objects 0.21 ± 0.01).

fMRI Experiment
During fMRI, stimuli were presented at 1 Hz in 12 s blocks of images from a single subcategory, alternating with 12 s of a blank screen with a fixation. Subjects participated in two 396 s runs and viewed a total of 4 blocks per subcategory. Each image was presented once, except for random image pairs that repeated successively within a block (~17% of images).

1-Back Task. Subjects were instructed to fixate on a central red point and press a button when images repeated successively. Due to occasional button box malfunction, behavioral data were obtained in 9/12 children and 10/12 adults.

Analysis of Imaging Data

Data were analyzed with Matlab and our in-house software, *mrVista* (white.stanford.edu/software).

Structural MRI

In each subject high-resolution anatomical whole-brain images from 4 scans were averaged into one volume. Using ITK-SNAP (white.stanford.edu/software), white and gray matter were segmented. The cortical surface was grown to include 4 mm of gray matter, creating a uniform gray matter thickness. Thus any variations in the volume of gray matter measurements in our study reflect variations in cortical surface area.

Anatomical Partitions of the VTC
Anatomical partitions were individually defined in each subject's native space as shown in Figure 1H. The VTC was defined as a region between the lateral border of the occipito-temporal sulcus (OTS), the medial border of the parahippocampal gyrus (PHG) extending to the lingual gyrus, and the fundus of the posterior transverse collateral sulcus (ptCoS). The ptCoS reliably marks the anterior edge of hV4 (Witthoft et al. 2014), thus excluding early retinotopic visual areas (V1-hV4) from the VTC. We subdivided the VTC into a total of 12 partitions. In the lateral to medial direction these partitions were: (1) the lateral fusiform gyrus (lFG) extending from the OTS to a line bisecting the midfusiform sulcus, (Nasr et al. 2011; Weiner et al. 2014)); (2) the medial FG (mFG), from the bisecting line of MFS to the lateral edge of the CoS, (3) the collateral sulcus (CoS) and (4) the PHG. Then we subdivided each of these partitions from posterior to anterior along the 20%, 40%, and 60% length of the VTC measured from the ptCoS to the temporal pole. The 40% boundary of the VTC coincided with the posterior limit of the hippocampal gyrus in both children and adults. Anatomical regions of interest (ROIs) were created by GG and validated by KGS.

There were no between age-group differences in the total volume of the right or left VTC or any of their partitions ($P > 0.3$), despite some trends towards "larger" volumes in children in some partitions (Fig. 1H). Also, the volume of the left VTC was larger in males than in females ($t_{(22)} = 2.86$, $P = 0.009$, t-test, data not shown), but there were no interactions among age and gender ($P > 0.18$) in the volume of the right or left VTC.

Functional MRI

Preprocessing
FMRI data were analyzed in each subjects' native brain space. For each subject, fMRI data were aligned to the 3D whole-brain volume and motion corrected. Data were detrended using a temporal high-pass filter with a 1/20 Hz cutoff. The time course of each voxel was converted to percent signal change by dividing its response amplitude at each TR by its mean amplitude across the time course. Data were not spatially smoothed.

General Linear Model
We used a standard general linear model (GLM) to generate voxel-by-voxel activation maps. Predictors were the stimulus conditions convolved with the hemodynamic impulse response function used in SPM (http://www.fil.ion.ucl.ac.uk/spm/). We estimated the beta coefficients for each stimulus category from a GLM applied to the preprocessed BOLD time series. We calculated several GLMs in each subject: (1) GLM of data from each run for MVP analyses (Figs 3 and 4, Supplementary Fig. 1), as well as independent analyses of response amplitudes (Fig. 6, Supplementary Fig. 7) and selectivity (Fig. 7) and (2) GLM using data from both runs to visualize activation maps and measure their volumes (Fig. 5, Supplementary Figs 2–6).

MVP Analyses
We determined the MVPs to each stimulus type within the anatomical boundaries of VTC separately for data from Run 1 and Run 2 (Fig. 3A) by calculating at each voxel the relative response amplitude to each stimulus type (1) as Z- score = $(\beta_i - E(\beta)/(\sigma/\sqrt{df}))$, where β_i is the β coefficient from the GLM for the ith stimulus, $E(\beta)$ is the

mean of all βs, σ is the square-root of the residual variance of the GLM and df is the degrees of freedom. Using Z-scores minimizes between-voxel differences in amplitudes, allowing estimation of category selectivity in each voxel, rather than amplitude differences across voxels (Sayres and Grill-Spector 2006).

Each MVP was represented as a vector of length n, where n is the number of voxels in each subject's anatomical ROI. For each subject we calculated the Pearson correlation coefficient (r) between MVPs from run1 versus run 2, for each pairing of stimulus types (i,j). Within-stimulus type correlations represent the reproducibility of the MVPs to a given category across runs (with different exemplars). Between-category correlations are a measure of similarity among MVPs to different stimulus types. Positive correlations indicate similar MVPs. Negative values indicate distinct MVPs. These correlations were averaged across subjects in each age group and displayed as a group averaged representational similarity matrix (RSM, Fig. 3B).

Test Between-Group Differences in the RSM by Bootstrapping
To examine statistical differences between RSMs of children versus adults we used bootstrapping. We tested the hypothesis that child and adult RSMs were different. That is, we tested whether the similarity among pairs of RSMs drawn from within-age groups (e.g., child$_i$ vs. child$_j$) was different than the similarity of RSMs drawn from across-age groups (e.g., child$_i$ vs. adult$_j$). We transformed each RSM to a vector and measured the Pearson correlation (r) among pairs of RSMs. Random pairs of RSMs were drawn with replacement from within an age group or across age groups by running 10 000 permutations. We transformed the Pearson correlation coefficient (r) to z-scores using the Fisher z-transformation to normalize the distribution of RSM similarities. We tested whether the mean of the within-group correlations were in- or outside of the 95% confidence interval of the distribution of between-group correlations. We also tested whether these distributions were different from the distribution of correlations among random pairs of RSMs from the entire pool of subjects. The results of bootstrap tests did not change when we examined the distribution of r or Fisher z-transformed data.

Classification of Visual Stimuli by A Winner-Take-All Classifier
We classified MVPs as corresponding to one of the 3 categories of faces, objects, or scenes (Fig. 3C, Supplementary Fig. 1A) or one of the 6 subtypes (Fig. 4, Supplementary Fig. 1B,C) of the stimuli that subjects viewed during fMRI. The winner-take-all classification was based on the highest similarity (Pearson correlation coefficient) between MVPs from a test run with each of the MVPs from a training run. We repeated this procedure for 2 permutations of test and training runs, averaged classification scores across both permutations per subject, and plotted the group-averaged data.

Activation Volumes
In each subject and anatomical partition, we measured the volume of activation for suprathreshold voxels based on data from 2 runs for the specified contrasts and thresholds (see GLM Methods above, Fig. 5, Supplementary Figs 2–6).

Individually Defined ROIs
All functional and anatomical ROIs were defined in each subject's individual native brain space, following the standard practice in the field (e.g., Malach et al. 1995; Kanwisher et al. 1996, 1997; Ishai et al. 1999; Haxby et al. 2001).

Independent Analysis of Response Amplitudes or Selectivity
In each subject, we applied a GLM to one run in order to define functional ROIs based on the contrast of interest. Then we applied a separate GLM to a second run, and estimated β values for each condition during fMRI. We repeated these steps for both permutations of independent analysis, averaged the estimated βs across the 2 permutations, and used these β estimates to calculate response amplitudes (percent signal change, Fig. 6, Supplementary Fig. 7) or selectivity (T-values, Fig. 7, Supplementary Fig. 8) at each voxel.

Independent Analysis of Selectivity (T-values) in Face-Selective Voxels (Fig. 7, Supplementary Fig. 8)
Face-selective voxels ([child + adult faces > cars + novel objects], $T > 3$) were defined and selectivity values were extracted in an independent analysis (see above). Selectivity was defined as the T-value for the relevant contrast, based on the β values and variance of the residual error from the independent GLM at each voxel. In each subject we measured the degree of selectivity for: (1) child faces versus objects, (2) adult faces versus objects, (3) cars versus scrambled objects, and (4) novel objects versus scrambled objects (Fig. 7). Selectivity data were averaged across both permutations of the independent analysis and across voxels of an ROI in each subject, and then averaged across subjects in each age group.

Statistical Methods
Subjects' data were averaged for each age group. Between-group differences were evaluated in SPSS20.0 (www.ibm.com) by 2-tailed repeated-measures analysis of variance (rmANOVA) or t-tests, unless otherwise noted.

In analyses of the volume of functional activations, subjects who showed no suprathreshold activation were assigned zero and included in the volume estimates. In analyses of response magnitude or selectivity, we excluded subjects for which we could not detect suprathreshold activations.

Controlling for Quality of BOLD Data Across Age Groups

A concern in pediatric neuroimaging is the potential effect of general factors that may differentially influence BOLD signals in children versus adults, leading to erroneous conclusions regarding the underlying neural processes. These include potential age-related differences in vasculature, metabolism, head size, distance to coil, subject's motion, signal-to-noise ratio, and reliability of the BOLD signals. Regarding metabolic and vascular responses, prior studies indicate that by age 7, (lowest age group in our study) these responses are not systematically different in children versus adults (Meek et al. 1998; Martin et al. 1999; Wenger et al. 2004), and unlikely to influence our results. Nevertheless, we evaluated several factors that could differentially influence BOLD measures across age groups, to ensure that subjects in different age groups were matched in terms of the quality of their BOLD data (Golarai et al. 2007; Grill-Spector et al. 2008). Thus, we compared age groups on the following measures:

1. *Motion:* Based on the estimated motion correction parameters we excluded subjects who moved more than one voxel during either scan. This led to the exclusion of 13 children and 1 adult. The remaining 12 children and 12 adults were matched in motion during fMRI (Fig. 1B).
2. *Brain to coil distance axial:* We controlled for any age-related differences in head size that might put children in a disadvantage in terms of BOLD measurements across the VTC. To estimate the proximity of the occipito-temporal cortex to the surface coil, in each subject's inplane anatomical scan we measured the shortest distance between the occipital

pole and the outer edge of the skull (Fig. 1C). The brain-to-coil distance was significantly higher in adults than in children ($t_{(22)} = 2.89$, $P = 0.01$; t-test) due to thicker skull and dura in adults. Thus, children's' brains were on average closer to the surface coil, resulting in a trend towards higher mean BOLD signals than adults (see below).

3. *Brain to coil distance coronal:* We estimated the proximity of the lateral cortex to the surface coil by measuring the shortest distance between the outer edges of the 2 ear canals in each subject from their in-plane anatomical scans. We found no between-group differences (Fig. 1D). Given that we used the same surface coil for all subjects in the study, these ear-to-ear measurements give a reliable (albeit indirect) estimate for the distance between brain to coil in the coronal axis.

4. *Mean BOLD signals in VTC:* To test for any differences across age-groups in (1) the spatial distortions caused by the ear canal artifact and (2) the overall mean signal, we measured in each subject the mean BOLD signal at each voxel, visualized signals on the cortical surface (Fig. 1F, example subjects), and calculated the average mean signal in each of the 12 anatomical partitions of the VTC in each subject. Then, we compared these mean BOLD signal measures across age groups. In general, the ear canal artifact was not different or smaller in children than in adults. Furthermore, mean BOLD signals were significantly higher in children's VTC than in adults', especially in the lateral and anterior VTC partitions in both hemispheres (right and left VTC: age of subject: $F_{1,110} > 25.48$, $P < 0.0001$; age of subject X partition: $F_{5,110} > 10.27$, $P < 0.004$; 2-way rmANOVA, data not shown). Higher mean BOLD signals in children than in adults, indicates that our use of surface coil put children at an advantage in terms of BOLD measurements across the VTC.

5. *Time series signal-to-noise ratio (tSNR):* tSNR during the blank baseline period was measured at each voxel as the mean signal divided by the standard deviation of the time series. The average tSNR across voxels were not significantly different across age groups (right and left VTC: age of subject: $F < 1.18$, $P > 0.2$, Fig. 1G). However, we found tSNR differences across VTC partitions (right and left VTC: partition: $F > 17.4$, $P < 0.0001$, Fig. 1G), as the susceptibility artifact around the ear canal significantly reduced tSNR in the anterior FG (Fig. 1F). Thus, we excluded the anterior VTC from further analyses, as it was below the minimal tSNR of 35, as previously suggested (Murphy et al. 2007).

6. *Reproducibility of MVPs across runs:* We tested the reproducibility of MVPs (based on the average Pearson correlation of MVPs) across different images of the same subcategory across

2 runs. We found no significant differences across age groups ($t_{(22)} < 1.9$, $P > 0.1$, t-test, Fig. 1E).

Results

The Quality of BOLD Signals During fMRI and Accuracy in the 1-Back Task are not Different Across Age Groups

We examined the development of VTC responses to faces, objects, and scenes across children and adults while subjects viewed images of these categories in blocks and performed a 1-back task (Fig. 1A, Materials and Methods). There were no significant differences among age groups in motion during fMRI, proximity to coil, reproducibility of distributed fMRI responses, or tSNR (Fig. 1B–G). Likewise, the volume of gray matter in the VTC was not significantly different across age groups (Fig. 1H). These measurements indicate that the quality of BOLD measurements were similar across age groups (Materials and Methods).

During the 1-back task, mean accuracy was high and not significantly different across age groups (Fig. 2A). There were no significant main effects of age, or interactions between age and stimulus category ($F < 1.36$, $P > 0.21$, 2-way rmANOVA, Fig. 2A), despite numerically lower accuracy for abstract objects, outdoor scenes and textures in children. Importantly, there were no between-group differences in accuracy across face subtypes (no main effect of age or age of subject × face subtype interaction, $F < 0.36$, $P > 0.55$).

Children had longer response times than adults across all stimulus types (main effect of age of subject: $F_{1,20} = 19.06$, $P < 0.0001$, 2-way rmANOVA, Fig. 2B), as expected from prior research (Kail and Salthouse 1994; Ratcliff et al. 2012; Cromer et al. 2015; Egami et al. 2015). However, there were no interactions between age of subjects and stimulus category (age of subject × category: $F_{6,102} = 0.13$, $P = 0.72$); and importantly, there were no significant differences in response times to own- versus other age faces (age of subject × face subtype: $F = 0.65$, $P = 0.43$, 2-way rmANOVA, Fig. 2B). These data indicate that children and adults were similarly responsive and accurate during the 1-back task on own- and other-age faces.

The Topology of Distributed Responses Across the VTC is Stable Across Age Groups

We asked if development is associated with changes in the spatial topology of distributed responses across the VTC. Thus, we examined MVPs of response to faces, objects, and scenes in each subject's VTC. We examined (1) the spatial organization of
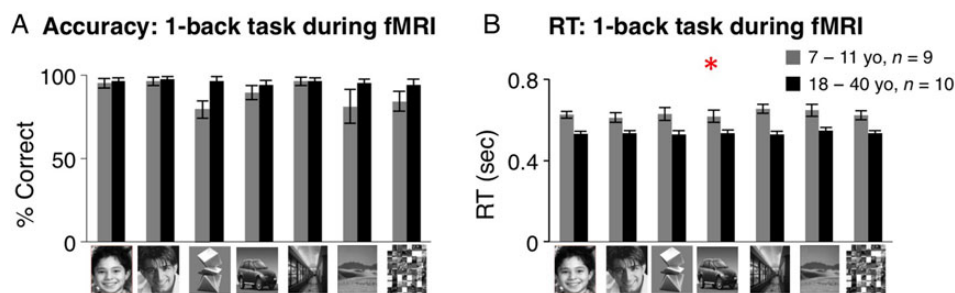

Figure 2. Behavioral performance on the 1-back task during fMRI. (A) Performance on the 1-back task during fMRI for children (gray) and adults (black) was highly accurate. There were no significant differences across age groups, or interactions between age and stimulus category across visual stimuli in mean accuracy. Results were similar when we considered responses to all visual stimuli, or just responses to faces. Error bars: group SEM. (B) Response times in the 1-back task during fMRI were significantly slower in children than in adults across all stimulus types. Error bars: group SEM. Asterisk: significant main effect of age group, $P < 0.0001$.

these MVPs with respect to major anatomical landmarks of VTC, and (2) the information content of these MVPs.

In children, faces, objects, and scenes evoked distinct MVPs, each with a characteristic spatial topology across the VTC (example child subject in Fig. 3A). Children's, MVPs to faces showed higher than average responses in the FG and lower than average responses in the medial VTC, overlapping the CoS and PHG. The reverse spatial topology was observed for scene MVPs. Distinct from responses to either faces or scenes, MVPs to objects showed greater than average responses in the medial FG, and less than average responses in both the lateral FG and medial VTC. This topology was robust, as it was evident in data from single fMRI runs in each child (e.g., Fig. 3A), and reproducible across 12 of 12 children that we tested. Importantly, the functional topology of VTC in children was qualitatively similar to adults' in our sample (see representative example in Fig. 3A) as well as to previously published data on adults (Haxby et al. 2001; Golarai et al. 2010; Weiner and Grill-Spector 2010). These findings suggest that the large-scale topology of the VTC responses to faces, objects, and scenes in children is similar to adults.

In children, MVPs to faces, objects, and scenes were highly similar within a category, but distinct across categories. To quantify

similarity, we calculated the Pearson correlation coefficient between all pairs of MVPs across Runs 1 and 2 in each subject, averaged across subjects, and summarized these averaged correlations in a RSM, separately for each age group (Fig. 3B). In children, different stimuli of the same category yielded similar MVPs that were positively correlated (within-category correlations: rVTC: 0.49 ± 0.02, lVTC: 0.47 ± 0.03, mean ± standard error of mean [SEM]). In contrast, stimuli of different categories yielded dissimilar MVPs (between-category correlations: rVTC: 0.14 ± 0.03, lVTC: 0.12 ± 0.02). The data in children were similar to the data observed in adults in which within-category correlations among MVPs (rVTC: 0.55 ± 0.03; lVTC: 0.56 ± 0.03) were higher than between-category correlations (rVTC: 0.14 ± 0.03; lVTC: 0.12 ± 0.02). Indeed, within-category MVPs were significantly more positively correlated than between-category MVPs in each hemisphere and age group (within- vs. between-category correlations: $t_{(11)} > 12.91$, $P < 10^{-3}$, paired t-test). Furthermore, the ranking of MVP correlations was similar across age groups. For example, MVPs to child faces were positively correlated with MVPs to adult faces. Also, face MVPs showed near zero correlations with object MVPs, and negative correlations with scene MVPs (Fig. 3B). Thus, the overall structure of the group RSM was qualitatively stable across age groups.
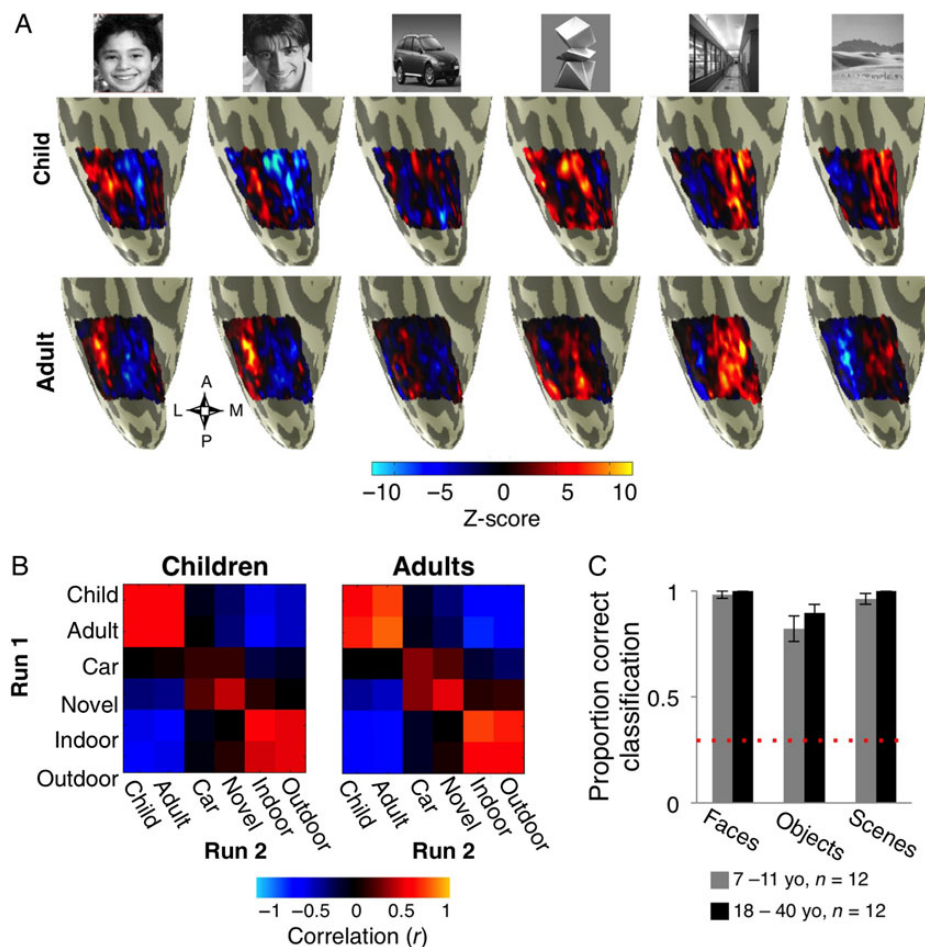
Figure 3. Multivoxel pattern (MVP) analysis of distributed responses across the right VTC in children and adults. (A) Visualization of the MVPs across the right VTC in response to each stimulus type during one run of fMRI from a representative 10-year-old child (top) and a 36 year-old adult (bottom). (B) RSM displays the Pearson correlation coefficients among all MVP pairs from Run 1 versus Run 2 across the entire VTC. Data are averaged across subjects from each age group (children, $n = 12$ and adults, $n = 12$). Each cell presents the group-averaged correlation among a pair of stimuli across runs. (C) Accuracy in decoding the category of the stimulus (face, object, or scene) from the MVP across the VTC by a winner-take-all classifier. Data are averaged across 12 children (gray) and 12 adults (black). Error bars: group SEM. Dashed red line: chance level classification.

The relative magnitudes of between-category correlations reflected the spatial topology of MVPs in both age groups. In children, the correlation between face- and object-MVPs was higher than the correlation between face- and scene-MVPs. This rank ordering of correlations was similar to adults', and tracked the topological organization of distributed responses across the VTC along its lateral-to-medial axis. That is, the peak responses to faces and objects were proximal, but the peak responses to faces and scenes were more widely separated (Fig. 3A). Thus, a developmentally stable large-scale functional topology of distributed VTC response to faces, objects, and scenes was associated with a qualitatively stable structure of the RSM for these categories across age groups.

To test for quantitative differences in the functional topology across age groups, we measured the similarity between RSMs among pairs of subjects within or across age groups in a series of bootstrap tests (see Materials and Methods). We reasoned that if development involves changes in RSMs, pairs of RSMs drawn from within an age group would be more similar than pairs drawn from across age groups. We found that the distribution of Fisher z-transformed Pearson correlations among pairs of RSMs drawn from within-age groups versus RSMs drawn from between-age groups were highly overlapping and thus statistically indistinguishable (within-age group: rVTC: children: 1.25 [0.73–2.07], mean [95% confidence interval of z-scores], adults: 1.45 [1.03–1.89]; lVTC: children: 1.20 [0.80–1.67], adults: 1.42 [0.92–2.00], between-age groups: rVTC: 1.33 [0.80–1.94], lVTC: 1.30 [0.88–1.79]). Likewise, we expected that large-scale developmental changes in RSMs would lead to a lower similarity between pairs of RSMs drawn across age groups than random pairs of RSMs from the entire pool of subjects. However, we found that the mean of between-age group correlations was numerically similar to the mean (and well within the 95% confidence interval) of the distribution of correlations among random pairs of RSMs drawn from the entire pool of subjects (between-age groups: rVTC: 1.33 [0.80–1.94] mean [95% confidence interval of z-scores]; lVTC: 1.30 [0.88–1.79]) random pairs: rVTC: 1.34 [0.79–1.95]; lVTC: 1.31 [0.86–1.84]). These findings confirm that the large-scale structure of RSM for distributed VTC responses to faces, objects and scenes is stable during development.

To quantify further the categorical information in the MVPs in each age group, we used a winner-take-all classifier on each subjects' MVPs. This classifier determined the categorical membership of the stimuli that the subject viewed during fMRI. The classifier accurately decoded if a child was viewing faces, objects, or scenes (accuracy in decoding children's MVPs > 92%, Fig. 3C). This classification performance was similar to that based on adults' MVPs (accuracy > % 96, Fig. 3C). For both age groups, classification accuracy varied across stimulus categories, and was higher for faces than for objects. A 2-way repeated rmANOVA on classification accuracy, using factors of stimulus category and age of subject, showed a significant effect of stimulus category in the right VTC (rVTC: stimulus category: $F_{2,44} = 3.67$, $P = 0.03$). However, there were no between age-group differences in the accuracy of these classifications or interaction between subject age and stimulus category (rVTC: age of subject: $F_{1,44} = 1.32$, $P > 0.26$, stimulus category × age of subject: $F_{2,22} = 2.2$, $P > 0.15$, Fig. 3C). Classification accuracy was similarly high in the left VTC, and there were no significant effects of age of subject, category, or interaction among these factors (Supplementary Fig. 1A). Thus, the categorical information content of distributed responses to faces, objects, and scenes across the VTC is developmentally stable after age 7.

Own- and Other-Age Faces are Differentially Represented Across the VTC

Although we found that age groups were similar in their large-scale representations of faces, objects and scenes across the VTC, the representation of subtypes of these categories may change with age and experience. Thus, we tested the hypothesis that more recent experience with own-age faces leads to different MVPs across the VTC for own- versus other-age faces. This hypothesis predicts that a classifier would decode the age of face stimuli more accurately from own- than from other-age face MVPs.

Accuracy in decoding MVPs in response to child and adult faces showed an own-age preference in adults. A 2-way rmANOVA on classification accuracy, with factors of age of subject and age of faces, revealed a significant interaction in the right VTC (age of subject × age of face: $F_{1,22} = 6.00$, $P = 0.02$; age of subject: $F_{1,22} = 1.6$, $P = 0.29$; age of face: $F_{1,22} = 6.0$, $P = 0.02$, Fig. 4A). This interaction was due to higher decoding accuracy of MVPs to adult versus child faces in adult participants (rVTC: $t_{(11)} > 3.63$, $P < 0.004$, paired t-test, Figure 4A). In contrast, in children decoding accuracy was similar for adult and child faces (rVTC: $t_{(11)} = 0.27$, $P = 0.79$, paired t-test). The differential representations of own- and other-age faces were distributed across the right VTC. That is, the interaction between the age of subject and age of face in decoding accuracy was not significant, when we restricted the decoder to a subset of voxels in the rVTC with either high face selectivity or no face selectivity (Supplementary Fig. 1B), or to voxels located in specific anatomical compartments of the FG (data not shown).

In the left VTC, we also found higher decoding accuracy for own- than for other age faces in adults (lVTC: $t_{(11)} = 2.8$, $P = 0.02$, paired t-test, Figure 4B) along with similar decoding of age of faces in children. However, differences in classification performance across age groups were not significant, and there were no significant interactions between age of subject and age of faces ($F < 1.4$, $P > 0.2$). Distinct from the right VTC, in the left VTC better classification of own- versus other-age faces was significant only when the classifier was restricted to the subset of face-selective voxels (Supplementary Fig. 1C).

In contrast to the differential decoding accuracy of own- versus other age faces, we did not find significantly different decoding of object or scene subtypes across age groups. In the rVTC, decoding accuracy for both object and scene subtypes was higher than chance (Fig. 4A), and decoding accuracy for indoor scenes was higher than outdoor scenes (scene subtype: $F_{1,22} = 3.97$, $P = 0.03$, 2-way rmANOVA, Fig. 4A). However, there were no significant effects of age of subject or interactions between age of subject and stimulus subtype in decoding accuracy for cars versus novel objects or for indoor versus outdoor scenes in either hemisphere (rVTC and lVTC: $F_{1,22} < 0.34$, $P > 0.57$, 2-way rmANOVA, Fig. 4A,B). Together, these data suggest a developmental differentiation in the distributed representations of own- and other-age faces that was more pronounced than developments in representation of subtypes of objects and scenes.

The Volume of Face-Selective Regions Develops Regardless of the Age of Face Stimuli, and Against a Stable Topology

The differential representation of own- versus other-age faces in the VTC raises the possibility that experience also shapes the development of face selectivity. Thus, we examined 4 facets of the development of face selectivity in the VTC: (1) the spatial extent of face-selective regions, (2) the spatial organization of face-
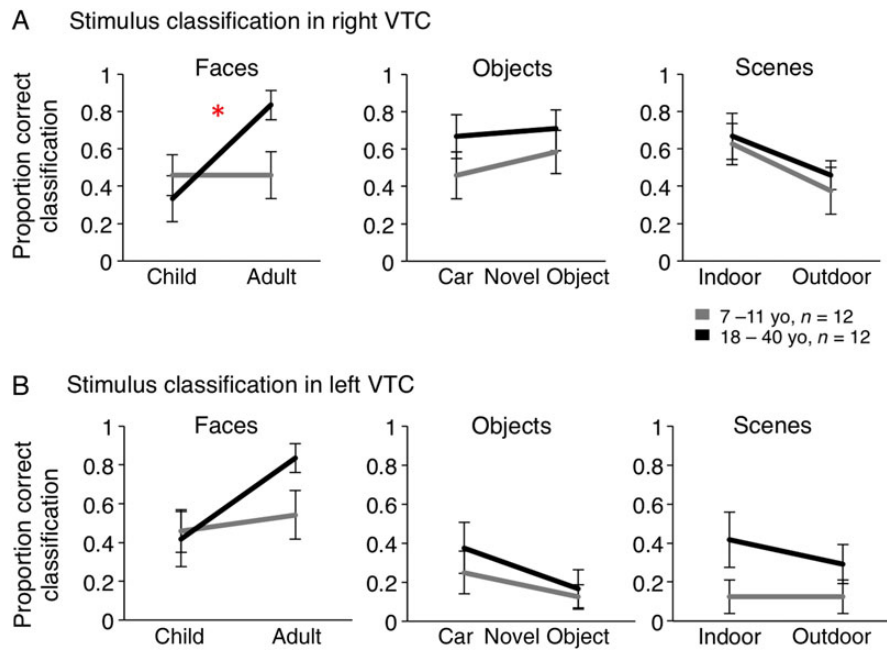
Figure 4. Accuracy in decoding MVPs to subtypes of faces, objects and scenes in the right (A) and left VTC (B) by a winner-take-all classifier. Data are averaged across 12 children (gray) and 12 adults (black). Error bars: group SEM. Chance level for classification is 16.67%. Asterisk: significant interaction between age of subject and age of face stimuli in decoding accuracy (P = 0.02).

selective voxels with respect to sulci and gyri of VTC, (3) their response amplitudes to visual stimuli, and (4) their magnitude of selectivity for own- versus other-age faces. We hypothesized that with experience, selectivity for own-age faces may undergo a more substantial development than for other-age faces. Alternatively, an age-related process may lead to a uniform development of selectivity for both subtypes of faces.

First, we asked if the spatial extent of face-selective regions develops with age or as a result of experience with own-age faces. Experience might lead to a larger volume of activation for own- than for other-age groups. Alternatively, an age-related development would be evident as larger volume of face-selective activations in adults than in children, regardless of the age of face stimuli. Note that these possibilities are not mutually exclusive, as both effects may co-occur. We also tested whether the development of face activations is associated with a spatial reorganization of face-selective regions, for example, a relocation of face-selective voxels from the medial VTC (CoS and PHG) to the lateral VTC (i.e., lFG and mFG), as previously reported (Gathers et al. 2004). Thus, we divided the VTC into 8 partitions based on the local gyri and sulci in each subject, as outlined in Figure 5A (also see Fig. 1H, Materials and Methods), and in each anatomical partition we measured the volume of activations that were selective for child faces [child faces > objects, T > 3], or for adult faces [adult faces > objects, T > 3] (Fig. 5A).

In children, selective activations to either child or adult faces were mostly located in the lFG, and to a lesser extent in the mFG. In contrast, the volume of face-selective activation was low in the medial VTC (CoS and PHG). This lateral-to-medial gradient of face-selective activation was more pronounced in the mid VTC (Fig. 5B) than in the posterior VTC (Fig. 5D), as activation volumes were also higher in the mid FG than in the posterior FG in both age groups. Qualitatively, the spatial organization of face-selective activation in children (Fig. 5B,D) was similar for own- and for other-age faces, and also similar to that in adults (Fig. 5C,E). However, in adults the volume of face-selective activation in the FG

was about twice higher than in children. Thus, the lateral-to-medial gradient of face-selective activation was more pronounced in the mid (Fig. 5C) and posterior VTC (Fig. 5E). A 3-way ANOVA with factors of age of subject, age of face stimuli, and anatomical partition (8 partitions outlined in Fig. 5A) showed significant main effects of age of subject and anatomical partition, and a significant interaction between age of subject and partition (rVTC: age of subject: $F = 11.78$, $P = 0.001$, partition: $F = 13.19$, $P < 0.0001$, age of subject × partition: $F = 2.13$, $P = 0.05$, 3-way rmANOVA). However, there were no significant effects of age of face stimuli or interactions between age of subjects and age of faces, or any other 2- or 3-way interactions ($F < 1.17$, $P > 0.28$).

Importantly, the age-related increase in the volume of face-selective activations occurred regardless of the age of face stimuli. A series of post hoc analyses showed that the volume of face-selective activations in the FG were higher in adults than in children both for child faces (by a factor of 2.2, $t_{(22)} = 2.58$, $P = 0.01$, t-test), and adult faces (by a factor of 1.9, $t_{(22)} = 3.04$, $P = 0.003$, t-test).

The age-related increase in the volume of face-selective activations occurred differently along the lateral to medial axis of the VTC. Namely, the volume of face activations (combined across age of faces) was higher in the right lFG and mFG of adults than of children, by a factor of 2.4 and 4.72, respectively ($t_{(22)} > 1.8$, $P < 0.03$, t-test). In contrast, the combined volume of face-selective activations (across age of faces) in the CoS and PHG were similarly low in both age groups (although numerically higher in adults than in children by a factor of 1.5, $t_{(22)} = 0.99$, $P = 0.33$ t-test). These data suggest that the developmental increase in face-selective activations was localized to the FG, where most face-selective voxels reside in both age groups, and could not be explained by a spatial reorganization of face-selective voxels along the lateral-medial axis of VTC.

We found a similar age-related increase in the volume of face-selective activations in the left hemisphere, but no significant 2- or 3-way interactions (Supplementary Fig. 2). These results replicated when we defined face selectivity by other contrasts,
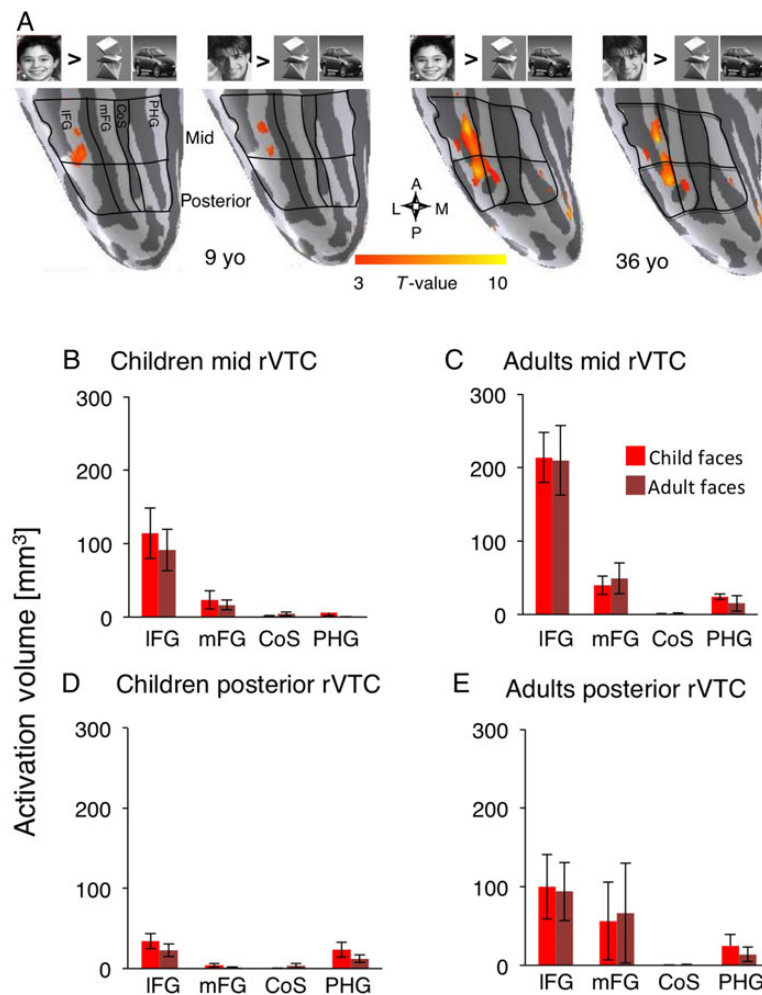
Figure 5. Volume of face-selective activations across the rVTC partitions. (A) Anatomical partitions and face activations are rendered on the surface of the right VTC from representative 9- and 36-year-old subjects. Face activations were defined based on selectivity for child faces versus objects ([child faces > cars + novel objects], T > 3); or selectivity for adult faces versus objects ([adult > car + objects], T > 3). The volumes of these activations were separately measured in each anatomical partition. (B–E) The total volume of activation to child faces (light bars) and to adult faces (dark bars) is plotted for the lateral fusiform gyrus (lFG), medial fusiform gyrus (mFG), collateral sulcus (CoS), and parahippocampal gyrus (PHG) in the right VTC (rVTC) averaged across 12 children (B,D) and 12 adults (C,E). (B,C) Data from the mid VTC, (D, E) from the posterior VTC. Error bars: group SEM.

including activations that were exclusively selective for child faces, exclusively selective for adult faces (Supplementary Fig. 3), or by contrasting faces against a variety of nonface stimuli, and across a range of thresholds (Supplementary Fig. 4).

Notably, in contrast to the age-related increase in the volume of face activations, the volume of activation for novel objects decreased with age and was 30–50% lower in the mid FG of adults than in children (Supplementary Figs 5 and 6). Thus, the developmental increase in the volume of face-selective activations does not reflect an increase in the volume of activation to all visual stimuli due to a general age effect.

Taken together, these data reveal a substantial age-related increase in the volume of face-selective regions that occurred irrespective of the age of face stimuli, and was localized to the FG, against a stable large-scale spatial organization of face-selective voxels across the VTC.

Response Amplitudes and Selectivity of Face-Selective Activations Show an Own-Age Bias

We tested whether age and experience shape the response amplitudes of face-selective regions in the FG. We hypothesized that general age-related developments would lead to changes in response amplitudes for both face subtypes, not excluding the possibility that differential experience with child or adult faces may lead to higher response amplitude for own- compared with other-age faces. In each subject we defined face-selective regions (child face + adult face > object, T > 3) from one run, and extracted from an independent run the response amplitude for each category of visual stimuli (Materials and Methods). Due to the relatively small volume of face-selective activations in the medial FG in both age groups, we combined the lateral and medial FG partitions into a single compartment (Fig. 6A).

Response amplitudes to both child and adult faces were higher in adults than in children (Fig. 6B–E). In contrast, responses to novel objects, scenes, and scrambled images were not different across age groups. A 3-way rmANOVA on the response amplitudes in the right FG, with factors of age of subject, stimulus type (6 stimuli), and compartment (posterior/mid), showed significant main effects of age of subject, stimulus type, and a 3-way interaction in the right FG (right FG: age of subject: $F_{1,21} = 8.2$, $P = 0.007$; stimulus type: $F_{1,110} = 55.69$, $P < 10^{-4}$; age of subject × stimulus type × partition: $F_{5,110} = 4.18$, $P = 0.04$, Fig. 6C,E). These
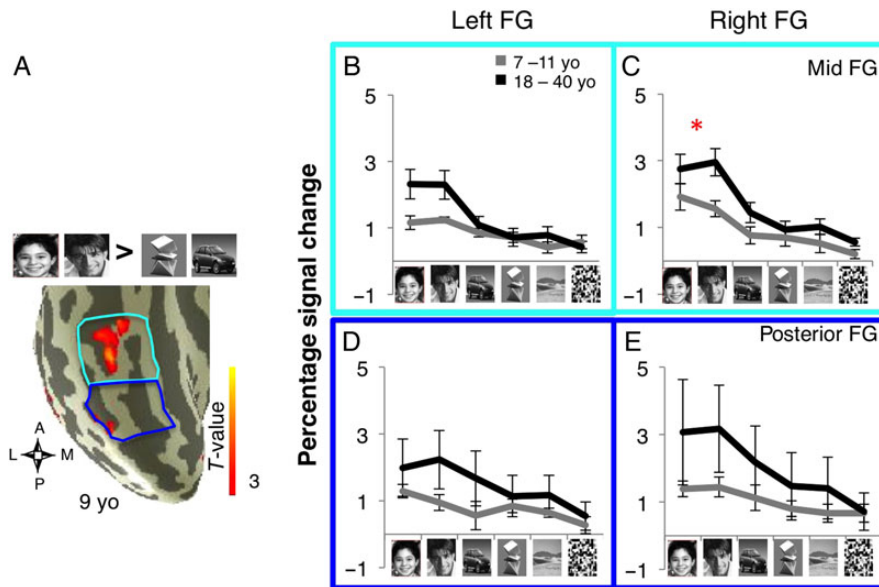
Figure 6. Response amplitudes of face-selective voxels in the FG in children and adults. (A) Anatomical partitions and face activation rendered on the cortical surface of the rVTC from a representative 9-year-old subject. The lFG and mFG partitions were combined to generate a compartment in the mid FG (cyan) and the posterior FG (blue). (B–E) Independent analysis of response amplitudes of face-selective voxels to visual stimuli in each FG compartment of right and left FG are plotted in units of percentage signal change. Face-selective voxels were defined based on the contrast ([child + adult faces > cars + novel objects], $T > 3$) in one run, and percentage signal change to stimuli was extracted from another run, and calculated relative to a blank baseline. Data were averaged across both iterations across the 2 runs in each subject, and then averaged across 11 children (gray, one child had no face-selective voxels in the mid FG) and 12 adults (black). Error bars: group SEM. (B,D) Left FG. (C,E) Right FG. Panels are colored by partition (see A) Asterisk: significant age of subject × age of face stimuli for percentage signal change in mid rFG: $P = 0.04$.

data show that response amplitudes of face-selective regions in the right FG increased with the age of subject, but not uniformly across stimuli or FG compartments.

To test further whether response amplitudes to faces undergo development, we carried out a series of post hoc tests on response amplitudes to own versus other-age faces, separately in each of the right FG compartments. We found higher response amplitudes to faces in adults than in children in each of the mid and posterior rFG compartments (age of subject: $F > 3.47$, $P < 0.04$, 2-way rmANOVA). In the mid rFG we also found a significant interaction between age of subject and age of faces (age of subject × age of face: $F_{1,22} = 4.19$, $P = 0.04$, 2-way rmANOVA, Fig. 6C), but not in the posterior rFG, (age of subject × age of face: $F = 0.015$, $P = 0.90$, 2-way rmANOVA, Fig. 6E).

In the left FG, a similar series of analyses showed an age-related increase in the response amplitudes to faces (age of subject: $F_{1,21} = 8.55$, $P = 0.005$, 3-way ANOVA). However, there was no evidence of an own-age preference (age of subject × age of face: $F_{1,21} = 0.85$, $P = 0.45$, 3-way rmANOVA) or any other 2- or 3-way interactions ($F < 1.7$, $P > 0.2$). These data reveal an age-related increase in response amplitudes to faces in the FG bilaterally, and an own-age preference in the mid rFG.

Based on these findings, we hypothesized that the development of face-selective regions is also associated with an age-related increase in the magnitude of selectivity for faces, especially for own-age faces. To test this possibility, we calculated the magnitude of selectivity for each face subtype (mean T-values for each face subtype: [child face > objects]; [adult face > objects], see Materials and Methods).

Consistent with the results on the response amplitudes to faces, we found an age-related increase in the magnitude of face selectivity across the entire FG, as well as higher selectivity for own- versus other-age faces in the mid rFG (Fig. 7A). A 3-way rmANOVA on the magnitude of face selectivity in the rFG,

with factors of age of subject, age of face stimuli, and anatomical compartment (mid/posterior), showed a significant effect of age of subject (age of subject: $F_{1,21} = 8.26$, $P = 0.006$) that varied with the age of faces and anatomical compartment (age of subject × age of face × FG compartment: $F_{1,21} = 4.68$, $P = 0.042$). However, other main effects or interactions were not significant ($F_{1,21} < 0.47$, $P > 0.5$). Post hoc 2-way ANOVAs on the magnitude of face selectivity (factors of age of subjects and age of faces), separately in each of the mid and posterior rFG compartments, revealed an interaction between age of face stimuli and age of subjects that was significant only in the mid rFG (age of subject × age of face: $F_{1,21} = 11.75$, $P = 0.002$), but not in the posterior rFG (age of subject × age of face: $F_{1,21} = 0.02$, $P = 0.90$). The interaction in the mid rFG was driven by significantly higher selectivity for own- versus other-age faces in both age groups (own- vs. other-age faces: $t_{(11 \text{ or } 12)} > 2.35$, $P < 0.05$, paired t-test). This own-age preference was observed in most adults ($n = 9/12$) and in about half the children ($n = 6/11$; one subject did not have suprathreshold face-selective voxels in mid rFG).

Among face-selective voxels of the left FG, we found significantly higher magnitude of face selectivity in adults than in children; however there was no evidence of an own-age preference in the magnitude of face selectivity (Supplementary Fig. 8A).

Together, these data reveal an own-age preference in the response amplitudes to faces and the magnitude of face selectivity, particularly in the mid rFG, along with an age-related increase in response amplitudes and selectivity to both face types across the posterior and mid FG, bilaterally.

Experience Modulates Responses of Face-Selective Regions to Nonface Stimuli

Do age and experience modulate responses of face-selective regions to nonface stimuli? Given that face-selective voxels in the FG responded more strongly to objects than to scrambled stimuli
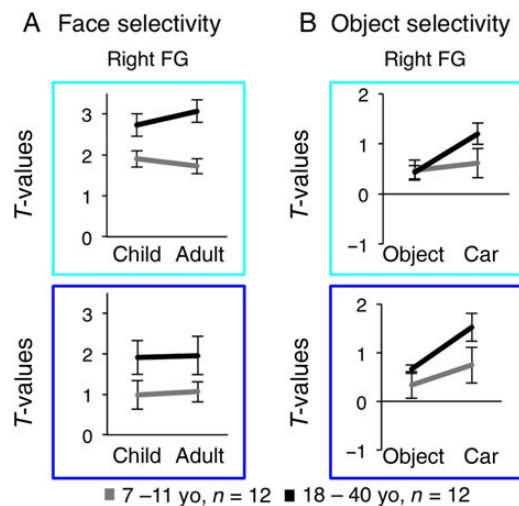
Figure 7. Magnitude of face and object selectivity in face-selective voxels of the FG in children and adults. (A) Independent analysis of the magnitude of selectivity of face-selective voxels (as in Fig. 6) to child faces (t-value for the contrast [child faces > novel objects + cars]) or adult faces (t-value for the contrast [adult faces > novel objects + cars]) in the mid (cyan) and posterior (blue) FG compartments of the right and left hemisphere. Data are averaged across 11 children (gray) and 12 adults (black). Error bars: group SEM. Asterisk: significant interaction between age of subject × age of face stimuli, P = 0.002. (B) Independent analysis of the magnitude of selectivity of face-selective voxels to cars (t-value for the contrast of cars > scrambled) and novel objects (t-value for the contrast novel objects > scrambled cars). Same subjects and ROIs as in (A).

(Fig. 6), and adults have more cumulative experience with cars than with novel objects, we asked whether response amplitudes for objects also varied with age and experience.

We found that response amplitudes of face-selective voxels in the rFG were higher to cars than to novel objects in adults (Fig. 6C,E). A 3-way rmANOVA on the amplitude of responses of face-selective voxels in the rFG to objects with factors of age group, object subtype (car/novel object), and FG compartment (mid/posterior), revealed differential responses to object subtype (object subtype: $F_{1,21} = 18.18$, $P < 0.0001$) that varied across age groups (age of subject × object subtype: $F_{1,21} = 5.75$, $P < 0.02$). However, other main effects or interactions were not significant ($F < 0.92$, $P > 0.35$). The interaction between age of subject and object subtype was driven by higher response amplitudes to cars than to novel objects in the right FG in adults (car vs. novel object: $t_{(11)} = 6.5$, $P < 0.0001$, paired t-test), but not in children (car vs. novel object: $t_{(11)} = 1.13$, $P = 0.27$, paired t-test). In contrast to the rFG, among face-selective voxels of the left FG, response amplitudes to cars and novel objects were not significantly different across age groups or FG compartments ($F < 1.9$, $P > 0.17$, Fig. 6).

Consistent with these findings, the magnitude of selectivity to cars (car vs. scrambled) was higher than to novel objects (novel object vs. scrambled) among the face-selective voxels of the rFG in adults (Fig. 7B). A 3-way rmANOVA on the magnitude of object selectivity in the right FG with factors of age group, object subtype (car/novel object), and FG compartment (posterior/mid) revealed higher selectivity in adults than in children (age of subject: $F_{1,21} = 4.74$, $P = 0.04$) and differential selectivity for object subtypes across age groups (age of subject × object type: $F_{1,21} = 11.13$, $P = 0.002$). However, other main effects or interactions were not significant ($F < 2.3$, $P > 0.14$). The interaction between age of subject and object subtype was driven by higher selectivity for cars than for novel objects in the rFG of adults (car vs. novel object: $t_{(11)} = 7.08$, $P < 0.0001$, paired t-test), but not children (car

vs. novel object: $t_{(11)} = 1.21$, $P = 0.24$, paired t-test, Fig. 7B). These data reveal higher selectivity for cars than for novel objects among face-selective voxels of the rFG in adults, but not in children.

In the left FG, selectivity for car stimuli was higher than for novel objects, but there were no significant effects of age of subject or any other main effects or interactions (Supplementary Fig. 8B).

Together, these data suggest that the response properties of face-selective regions may be modulated by years of experience with a nonface common object category, such as cars, and this effect is pronounced in the right FG.

Discussion

Our findings suggest that experience and age together shape the neural mechanisms of face processing in the VTC during a prolonged development that continues well after age 7. We found new evidence for an age-related differentiation in the representation of own- versus other-age faces. This differentiation manifested in 2 aspects of BOLD responses: (1) in the information content of distributed VTC responses, which was associated with more accurate decoding of MVPs for own- than for other-age faces in adults, and (2) in larger response amplitudes and higher selectivity for own- than other-age faces in face-selective regions of the mid FG which overlaps with mFus-faces/FFA-2 (Weiner and Grill-Spector 2010). Importantly, the differential representation of own- versus other-age faces was more pronounced in adults than in children, suggesting that more cumulative experience, and/or greater social salience of own-age faces in adults shape face representations. We also observed an age-related increase in the spatial extent of face-selective activations, as well as an age-related increase in their response amplitude to faces and magnitude of face selectivity. However, these developments occurred regardless of the age of face stimuli. These different measures of face-responsiveness and selectivity are related; as developments in responsiveness to faces would likely generate both higher selectivity and a larger spatial extent of suprathreshold voxels. In contrast to these prolonged developments, the large-scale spatial topology of face-, object-, and scene-selective activations relative to each other and to anatomical landmarks of VTC was stable across age groups. These findings suggest that an age-related differentiation in the representation of face subtypes is superimposed on an age-related increase in the spatial extent and magnitude of face selectivity, which occur over a relatively stable, large-scale, functional topology of distributed representations of faces, objects, and scenes in the VTC.

Several aspects of our methodology afforded a high level of confidence and precision in our findings. First, our results were not due to differences in the variability among child versus adult face stimuli, as the levels of pixel-wise similarities within these subtypes of face stimuli were equal (Materials and Methods). Second, age groups performed similarly across face stimuli in a 1-back task during fMRI, suggesting equal engagement with the face stimuli (Fig. 2A,B). Third, we optimized the quality of BOLD measurements across age groups by using a surface coil, which provided high SNR for the occipital and temporal cortices. Fourth, our controls indicate that the developmental findings in our study are not due to systematic across-group differences in BOLD measurements. Importantly, the average motion, tSNR, and reproducibility of BOLD responses were matched across age groups, ensuring similar quality of fMRI measurements across age groups (Fig. 1B–G). Furthermore, the larger volume of

activations to novel objects in the FG of children (compared with adults) rules out any substantial contribution of BOLD confounds in driving the specific developmental increases in the spatial extent amplitude and selectivity of responses to faces in the FG. Fifth, we enhanced the spatial precision of our measurements by examining developmental effects in VTC partitions, which were based on major anatomical landmarks in each subject (Fig. 1*H*). Together, these methodological controls ensured that general between-group differences, such as task performance during scan (due to differences in attention, anxiety, or motivation), BOLD related confounds or anatomical developments could not explain our findings.

Below, we discuss the implications of 3 aspects of our findings: (1) the stable topology of VTC categorical representations after age 7; (2) age-related changes in response to faces irrespective of the face subtype, and (3) experience-dependent changes in response to face and object subtypes.

The Topology of Face, Object, and Scene Representations is Stable After Age 7

Our data revealed the large-scale spatial topology of distributed responses to broad categories of faces, objects, and scenes in the VTC of children. This topology was highly reproducible in children, both in relation to major anatomical landmarks of VTC and in terms of the information content of the distributed responses to these broad categories (Fig. 3).

The topology of distributed responses in VTC was stable across age groups, both qualitatively, in terms of the large-scale spatial organization, and also quantitatively, in terms of their information content (Fig. 3). These findings suggest that the large-scale functional topology of face, object, and scene categories in VTC develops before age 7.

Developmentally, this topology may arise from a combination of factors, including (1) anatomical constraints, such as the cytoarchitecture of VTC (Caspers et al. 2012, 2014; Weiner et al. 2014), (2) long-distance white-matter connections (Gschwind et al. 2012; Phillips et al. 2012; Harel et al. 2013; Saygin et al. 2013; Gomez et al. 2015), and (3) functional constraints, such as eccentricity bias (Levy et al. 2001; Hasson et al. 2002) or responsiveness to primitive shapes (e.g., curvature vs. rectilinearity (Srihasam et al. 2012, 2014; Nasr et al. 2014)). Notably, each of these anatomical and functional factors is organized along the lateral-medial axis of VTC (Grill-Spector and Weiner 2014).

Our finding of a stable spatial topology of face-selective activations (Fig. 5, Supplementary Figs 2–4) argues against the idea that face-selective regions undergo a major relocation during childhood (Gathers et al. 2004). Also stable was the spatial location of activations for own- and other-age faces across 8 anatomical partitions of VTC, (Fig. 5, Supplementary Figs 2–4). In fact, the majority of face-selective voxels showed selectivity for both own- and also other-age faces (Supplementary Fig. 3).

The stable large-scale topology of face, object, and scene representations does not rule out the possibility of developmental changes in the representation of other categories or subcategories that were not included in our study. Future studies are needed to compare the development of a broader range of face and object representations, using a wider variety of stimulus categories that activate the VTC (e.g., animals, tools, body parts, or words) and subcategories (e.g., animal vs. human faces, kitchen utensils vs. construction tools) and tasks, to determine whether those VTC representations change during development. Based on our findings, we predict that the large-scale topology of category representations develops before the fine-grain distinctions among subtypes.

Face-Selective Regions Undergo An Age-Related Development Regardless of the Age of Faces

Despite a stable, large-scale functional topology, the spatial extent and magnitude of face selectivity in the FG increased after age 7, consistent with previous data from our studies and others' (Gathers et al. 2004; Golarai et al. 2007, 2010; Scherf et al. 2007; Peelen et al. 2009; Cantlon et al. 2011). Importantly, this age-related development (1) occurred regardless of the age of face stimuli (Fig. 5, Supplementary Figs 2 and 3), (2) was evident across a range of contrasts and statistical thresholds (Supplementary Fig. 4), and (3) was specific to faces and not found for objects (Supplementary Figs 5 and 6), ruling out a general maturation effect. Interestingly, in the same anatomical regions of FG—where we found a near doubling of the extent of face-selective activations with age—we also found a near 30% decrease in the extent of object-selective activations with age. These findings raise the intriguing possibility that with age and experience, some object-selective voxels in the FG (which are also responsive to faces, see Supplementary Fig. 7), may become face-selective, and contribute to the growth of the spatially expanding face-selective regions during development. This hypothesis may be examined in future longitudinal studies of development.

Several underlying neural mechanisms have been proposed to explain the development of face selectivity: (1) increased firing rate of face-selective neurons in response to faces (Grill-Spector et al. 2008; Srihasam et al. 2014), (2) reduced responsiveness to objects (Cantlon et al. 2011), (3) clustering of face-selective neurons in the FG due to large-scale functional reorganization of VTC (Gathers et al. 2004) or (4) clustering of face-selective neurons at the voxel level, all of which could lead to an age-related, net increase in face selectivity in the FG. Our data rule out a reduced responsiveness to objects among face-selective regions or a large-scale spatial reorganization in the VTC. Instead, our findings support age-related increases in responsiveness to faces within face-selective regions. Future studies with higher resolution fMRI or adaptation methods are needed to determine whether this development is due to greater clustering of face-selective neurons, increased responsiveness to faces, or both.

Experience-Dependent Differentiation in Representations of Own- Versus Other-Age Faces

A key finding in our study was an own-age advantage, which can be understood in terms of the role of experience in shaping 2 specific aspects of VTC responses. First, the distinct representation of own- compared to other-age faces in the distributed responses of VTC suggests that experience with peer faces shapes these representations, especially in adults. This plasticity was specific to distributed representation of faces and was not a general maturation effect, as we did not find an analogous interaction between age of subject and subtypes of objects or scenes (Fig. 4). Second, in both age groups the selectivity and amplitude of responses to own-age faces were higher than to other-age faces in face-selective voxels of the right mid FG (which corresponds to mFus-faces/FFA-2; (Weiner and Grill-Spector 2010). These data suggest that experience with own-age faces increases the local selectivity and response amplitudes for own-age faces in mFus-faces/FFA-2. However, we cannot rule out a less pronounced effect of this experience on the responses of face-selective regions in the posterior or left FG. Also, this own-age advantage was evident in both age groups, suggesting that in adults, recent years of experience with adult peers leads to a reversal of an earlier preference for childhood peers. These findings are consistent with reports of higher

FFA responses to own-race versus other-race faces (Golby et al. 2001) and suggest a flexible representation of face subtypes in the mFus-faces/FFA-2 well into adulthood.

What Components of Real Life Experience with Faces Contribute to the Own-Age Preference in VTC Responses?

We hypothesize that the relative frequency and cumulative effect of encounters with own- versus other-age faces, along with the greater social salience of own-age faces are critical factors (Cassia et al. 2009; Harrison and Hole 2009; Hills and Lewis 2011). For example, the combination of recent and cumulative experience would explain our observation of a larger own-age preference in distributed VTC representations in adults compared with children. Namely, adults typically interact socially with other adults on a daily basis, but not with many children. Meanwhile, adult faces dominate the social milieu throughout the life span and thus exert a cumulative effect since infancy (Macchi Cassia et al. 2014). In contrast, children's experience with peer faces is more transient as the physical shape of a child's face rapidly changes during development. Moreover, the asymmetric social salience and roles of adults versus children (e.g., in providing vs. receiving care) are likely to differentially shape the cumulative experience of children and adults with own- versus other-age faces.

One limitation of our study is that we did not quantify the timing, duration or frequency of our participant's prior experience with individuals of own- versus other-age groups. Thus, we cannot distinguish the contributions of ongoing, recent, or cumulative experience with own-age faces or the potential role of any "critical periods" during adolescence or early adulthood. Likewise, we did not attempt to change our subjects' level of experience by training our participants with other age faces, or by focusing on specific subpopulation of children (e.g., home schooled children) or adults (e.g., teachers) with more or less exposure to specific age groups. Future longitudinal studies before and after variable durations of every day exposure or laboratory training with different subtypes of faces are needed to test the specific effects of recent versus cumulative experience. However, our findings predict that prolonged and substantive experience with other ages will alter VTC responses to those face subtypes. For example, teachers or maternity ward nurses, who interact daily with children or infants, respectively, may show a decreased own-age preference in VTC responses relative to faces of the age group with which they have substantial daily experience, as suggested by behavioral studies (Cassia et al. 2009; Harrison and Hole 2009).

Responses in Face-Selective Regions are Also Malleable to Experience with Objects

Experience-dependent modulation of face-selective regions by nonface stimuli has been interpreted from divergent perspectives. One view suggests a unique and critical involvement of these regions in processing objects of expertise (Gauthier et al. 1999, 2000; McGugin et al. 2011; McGugin, Gatenby et al. 2012; Gauthier et al. 2014). A second view suggests that faces and objects are represented by nonoverlapping, domain-specific neural populations within an fMRI voxel (Kanwisher et al. 1997; Grill-Spector et al. 2004; McKone et al. 2007). A third-view posits a distributed representation of faces and objects allowing the possibility that experience with objects would affect response in face-selective regions (Haxby et al. 2001; Harel et al. 2013, 2014). A fourth view suggests that VTC responses are organized by combinations of shape (Nasr et al. 2014), animacy (Konkle and Caramazza 2013; Sha et al. 2015), and retinotopy (Levy et al. 2001). Given that cars and faces share some common features (e.g., rounded frontal features), these stimuli may generate activations at overlapping regions.

Our findings suggest that cumulative experience with a nonface object subtype (cars) shapes responses in face-selective regions. Specifically, the magnitude of selectivity and response amplitudes of face-selective regions in the adult FG were higher for cars (with which adults had many years of experience) than for novel objects (with which all subjects had little prior experience). Furthermore, in the same regions, responses to cars were higher in adults than in children, consistent with adults' greater cumulative experience with cars. In contrast, there were no age-group differences in the response of these regions to novel objects, ruling out a general maturation effect.

Preferential responses to cars overlapped the face-selective regions of mid rFG (i.e., mFus-faces/FFA-2), where we also found an own-age preference in response to faces. Future studies capable of resolving small neural populations are needed to determine whether the malleability to experience with face and nonface stimuli occurs among the same neuronal populations – as predicted by the expertise view (Gauthier et al. 2000; Gauthier and Bukach 2007; McGugin, Richler et al. 2012) – or among nonoverlapping populations within an fMRI voxel, as predicted by the domain-specificity view (Kanwisher et al. 1997; Grill-Spector et al. 2004; McKone et al. 2007).

Conclusions

We report 2 key findings. First, we find a sequential development of VTC, where the topology of distributed representations of faces, objects, and scenes developed by age 7, but the spatial extent and degree of face selectivity continued to develop into adulthood. Second, we provide the first direct evidence that experience plays a role in shaping the development of face representations in the VTC, as responses to own compared with other age faces became differentiated with age, both in the distributed responses of VTC and within face-selective regions. These findings elucidate the interplay of experience and maturation in shaping the development of the neural substrates of face processing in human VTC.

Supplementary Material

Supplementary material can be found at: http://www.cercor.oxfordjournals.org/.

Notes

References

Aylward EH, Park JE, Field KM, Parsons AC, Richards TL, Cramer SC, Meltzoff AN. 2005. Brain activation during face perception: evidence of a developmental change. J Cog Neuro Sci. 17:308–319.

Cantlon JF, Pinel P, Dehaene S, Pelphrey KA. 2011. Cortical representations of symbols, objects, and faces are pruned back during early childhood. Cereb Cortex. 21:191–199.

Caspers J, Zilles K, Amunts K, Laird AR, Fox PT, Eickhoff SB. 2014. Functional characterization and differential coactivation patterns of two cytoarchitectonic visual areas on the human posterior fusiform gyrus. Hum Brain Mapp. 35:13.

Caspers J, Zilles K, Eickhoff SB, Schleicher A, Mohlberg H, Amunts K. 2012. Cytoarchitectonical analysis and probabilistic mapping of two extrastriate areas of the human posterior fusiform gyrus. Brain Struct Funct. 218:15.

Cassia VM, Picozzi M, Kuefner D, Casati M. 2009. Why mix-ups don't happen in the nursery: evidence for an experience-based interpretation of the other-age effect. Q J Exp Psychol (Hove). 62:1099–1107.

Cromer JA, Schembri AJ, Harel BT, Maruff P. 2015. The nature and rate of cognitive maturation from late childhood to adulthood. Front Psychol. 6:704.

Egami C, Yamashita Y, Tada Y, Anai C, Mukasa A, Yuge K, Nagamitsu S, Matsuishi T. 2015. Developmental trajectories for attention and working memory in healthy Japanese school-aged children. Brain Dev. 37(9): 840–848.

Gathers AD, Bhatt R, Corbly CR, Farley AB, Joseph JE. 2004. Developmental shifts in cortical loci for face and object recognition. Neuroreport. 15:1549–1553.

Gauthier I, Bukach C. 2007. Should we reject the expertise hypothesis? Cognition. 103:322–330.

Gauthier I, McGugin RW, Richler JJ, Herzmann G, Speegle M, Van Gulick AE. 2014. Experience moderates overlap between object and face recognition, suggesting a common ability. J Vis. 14:7.

Gauthier I, Skudlarski P, Gore JC, Anderson AW. 2000. Expertise for cars and birds recruits brain areas involved in face recognition. Nat Neurosci. 3:191–197.

Gauthier I, Tarr MJ, Anderson AW, Skudlarski P, Gore JC. 1999. Activation of the middle fusiform 'face area' increases with expertise in recognizing novel objects. Nat Neurosci. 2:568–573.

Golarai G, Ghahremani DG, Whitfield-Gabrieli S, Reiss A, Eberhardt JL, Gabrieli JD, Grill-Spector K. 2007. Differential development of high-level visual cortex correlates with category-specific recognition memory. Nat Neurosci. 10:512–522.

Glover GH. 1999. 3D z-shim method for reduction of susceptibility effects in BOLD fMRI. Magn Reson Med. 42:290–299.

Golarai G, Liberman A, Yoon JM, Grill-Spector K. 2010. Differential development of the ventral visual cortex extends through adolescence. Front Hum Neurosci. 3:80.

Golby AJ, Gabrieli JDE, Chiao JY, Eberhardt JL. 2001. Differential responses in the fusiform region to same-race and other-race faces. Nat Neurosci. 4:845–850.

Gomez J, Pestilli F, Witthoft N, Golarai G, Liberman A, Poltoratski S, Yoon J, Grill-Spector K. 2015. Functionally defined white matter reveals segregated pathways in human ventral temporal cortex associated with category-specific processing. Neuron. 85:216–227.

Grill-Spector K, Golarai G, Gabrieli J. 2008. Developmental neuroimaging of the human ventral visual cortex. Trends Cogn Sci. 12:152–162.

Grill-Spector K, Knouf N, Kanwisher N. 2004. The fusiform face area subserves face perception, not generic within-category identification. Nat Neurosci. 7:555–562.

Grill-Spector K, Kushnir T, Edelman S, Avidan G, Itzchak Y, Malach R. 1999. Differential processing of objects under various viewing conditions in the human lateral occipital complex. Neuron. 24:187–203.

Grill-Spector K, Weiner KS. 2014. The functional architecture of the ventral temporal cortex and its role in categorization. Nat Rev Neurosci. 15:536–548.

Gschwind M, Pourtois G, Schwartz S, Van De Ville D, Vuilleumier P. 2012. White-matter connectivity between face-responsive regions in the human brain. Cereb Cortex. 22:1564–1576.

Harel A, Kravitz D, Baker CI. 2013. Beyond perceptual expertise: revisiting the neural substrates of expert object recognition. Front Hum Neurosci. 7:885.

Harel A, Kravitz DJ, Baker CI. 2014. Holding a stick at both ends: on faces and expertise. Front Hum Neurosci. 8:442.

Harrison V, Hole GJ. 2009. Evidence for a contact-based explanation of the own-age bias in face recognition. Psychon Bull Rev. 16:5.

Hasson U, Levy I, Behrmann M, Hendler T, Malach R. 2002. Eccentricity bias as an organizing principle for human high-order object areas. Neuron. 34:479–490.

Haxby JV, Gobbini MI, Furey ML, Ishai A, Schouten JL, Pietrini P. 2001. Distributed and overlapping representations of faces and objects in ventral temporal cortex. Science. 293:2425–2430.

Hills PJ, Lewis MB. 2011. The own-age face recognition bias in children and adults. Q J Exp Psychol (Hove). 64:17–23.

Ishai A, Ungerleider LG, Martin A, Schouten JL, Haxby JV. 1999. Distributed representation of objects in the human ventral visual pathway. Proc Natl Acad Sci USA. 96:9379–9384.

Kail R, Salthouse TA. 1994. Processing speed as a mental capacity. Acta Psychol (Amst). 86:199–225.

Kanwisher N, Chun MM, McDermott J, Ledden PJ. 1996. Functional imaging of human visual recognition. Brain Res Cogn Brain Res. 5:55–67.

Kanwisher N, McDermott J, Chun MM. 1997. The fusiform face area: a module in human extrastriate cortex specialized for face perception. J Neurosci. 17:4302–4311.

Konkle T, Caramazza A. 2013. Tripartite organization of the ventral stream by animacy and object size. J Neurosci. 33:10235–10242.

Kriegeskorte N, Mur M, Bandettini P. 2008. Representational similarity analysis - connecting the branches of systems neuroscience. Front Syst Neurosci. 2:4.

Levy I, Hasson U, Avidan G, Hendler T, Malach R. 2001. Center-periphery organization of human object areas. Nat Neurosci. 4:533–539.

Lewin C, Herlitz A. 2002. Sex differences in face recognition–women's faces make the difference. Brain Cogn. 50:121–128.

Macchi Cassia V, Bulf H, Quadrelli E, Proietti V. 2014. Age-related face processing bias in infancy: evidence of perceptual narrowing for adult faces. Dev Psychobiol 56(2):238–248.

Malach R, Reppas JB, Benson RR, Kwong KK, Jiang H, Kennedy WA, Ledden PJ, Brady TJ, Rosen BR, Tootell RB. 1995. Object-related activity revealed by functional magnetic resonance imaging in human occipital cortex. Proc Natl Acad Sci USA. 92: 8135–8139.

Martin E, Joeri P, Loenneker T, Ekatodramis D, Vitacco D, Hennig J, Marcar VL. 1999. Visual processing in infants and children studied using functional MRI. Pediatr Res. 46:135–140.

McGugin RW, Gatenby JC, Gore JC, Gauthier I. 2012. High-resolution imaging of expertise reveals reliable object selectivity in the fusiform face area related to perceptual performance. Proc Natl Acad Sci USA. 109:17063–17068.

McGugin RW, Richler JJ, Herzmann G, Speegle M, Gauthier I. 2012. The Vanderbilt Expertise Test reveals domain-general and domain-specific sex effects in object recognition. Vision Res. 69:10–22.

McGugin RW, Tanaka JW, Lebrecht S, Tarr MJ, Gauthier I. 2011. Race-specific perceptual discrimination improvement following short individuation training with faces. Cogn Sci. 35:330–347.

McKone E, Kanwisher N, Duchaine BC. 2007. Can generic expertise explain special processing for faces? Trends Cogn Sci. 11:8–15.

Meek JH, Firbank M, Elwell CE, Atkinson J, Braddick O, Wyatt JS. 1998. Regional hemodynamic responses to visual stimulation in awake infants. Pediatr Res. 43:840–843.

Murphy K, Bodurka J, Bandettini PA. 2007. How long to scan? The relationship between fMRI temporal signal to noise ratio and necessary scan duration. Neuroimage. 34:565–574.

Nasr S, Echavarria CE, Tootell RB. 2014. Thinking outside the box: rectilinear shapes selectively activate scene-selective cortex. J Neurosci. 34:6721–6735.

Nasr S, Liu N, Devaney KJ, Yue X, Rajimehr R, Ungerleider LG, Tootell RB. 2011. Scene-selective cortical regions in human and nonhuman primates. J Neurosci. 31:13771–13785.

Peelen MV, Glaser B, Vuilleumier P, Eliez S. 2009. Differential development of selectivity for faces and bodies in the fusiform gyrus. Dev Sci. 12:F16–F25.

Phillips JS, Greenberg AS, Pyles JA, Pathak SK, Behrmann M, Schneider W, Tarr MJ. 2012. Co-analysis of brain structure and function using fMRI and diffusion-weighted imaging. J Vis Exp. 69:4125.

Ratcliff R, Love J, Thompson CA, Opfer JE. 2012. Children are not like older adults: a diffusion model analysis of developmental changes in speeded responses. Child Dev. 83:367–381.

Saygin ZM, Norton ES, Osher DE, Beach SD, Cyr AB, Ozernov-Palchik O, Yendiki A, Fischl B, Gaab N, Gabrieli JD. 2013. Tracking the roots of reading ability: white matter volume and integrity correlate with phonological awareness in prereading and early-reading kindergarten children. J Neurosci. 33:13251–13258.

Sayres R, Grill-Spector K. 2006. Object-selective cortex exhibits performance-independent repetition suppression. J Neurophysiol. 95:995–1007.

Scherf KS, Behrmann M, Dahl RE. 2012. Facing changes and changing faces in adolescence: a new model for investigating adolescent-specific interactions between pubertal, brain and behavioral development. Dev Cogn Neurosci. 2:199–219.

Scherf KS, Behrmann M, Humphreys K, Luna B. 2007. Visual category-selectivity for faces, places and objects emerges along different developmental trajectories. Dev Sci. 10:F15–F30.

Sha L, Haxby JV, Abdi H, Guntupalli JS, Oosterhof NN, Halchenko YO, Connolly AC. 2015. The animacy continuum in the human ventral vision pathway. J Cogn Neurosci. 27:665–678.

Srihasam K, Mandeville JB, Morocz IA, Sullivan KJ, Livingstone MS. 2012. Behavioral and anatomical consequences of early versus late symbol training in macaques. Neuron. 73:608–619.

Srihasam K, Vincent JL, Livingstone MS. 2014. Novel domain formation reveals proto-architecture in inferotemporal cortex. Nat Neurosci. 17:1776–1783.

Weiner KS, Golarai G, Caspers J, Chuapoco MR, Mohlberg H, Zilles K, Amunts K, Grill-Spector K. 2014. The mid-fusiform sulcus: a landmark identifying both cytoarchitectonic and functional divisions of human ventral temporal cortex. Neuroimage. 84:453–465.

Weiner KS, Grill-Spector K. 2010. Sparsely-distributed organization of face and limb activations in human ventral temporal cortex. Neuroimage. 52:1559–1573.

Wenger KK, Visscher KM, Miezin FM, Petersen SE, Schlaggar BL. 2004. Comparison of sustained and transient activity in children and adults using a mixed blocked/event-related fMRI design. Neuroimage. 22:975–985.

Witthoft N, Nguyen ML, Golarai G, LaRocque KF, Liberman A, Smith ME, Grill-Spector K. 2014. Where is human V4? Predicting the location of hV4 and VO1 from cortical folding. Cereb Cortex. 24:2401–2408.